
Modular approach to high power density servo motor drivers with STSPIN32G4

By P. Lombardi, E. Poli



Abstract

The market for servo driving applications has stringent requirements in terms of form factor, power density, and reliability, which makes designing robust solutions challenging. STMicroelectronics recently published the [EVLSEVVO1](#), a very compact and powerful reference design addressing this segment. Thanks to system-level optimizations and the use of the STSPIN32G4, ST's STSPIN flagship device for 3-phase brushless DC, an extremely integrated and flexible motor controller with an embedded Cortex®-M4 microcontroller, it was possible to create an inverter capable of delivering 3 kW of power to the electric motor with solid switching and thermal performance.

The design is reinforced by several protections, based on both hardware and software, for maximum flexibility and complete coverage. These protections are designed to keep both the driver and motor in a safe state in case of anomalies. The [EVLSEVVO1](#) design is detailed in this paper, providing references and hints to application designers for building their best servo driving solutions. Experimental data are also included to demonstrate the exceptional results achievable.

1 Introduction

In recent years, there has been an increasing demand for high-power motor drive solutions. In particular, the field of low-voltage servo driving applications is pushing for reliable systems capable of managing significant power transfer to the electric motor, ranging from a few hundred to several thousand watts. This application field is dominated by 3-phase brushless motors thanks to their flexibility and strong performance, both in terms of positioning and torque regulation applied to the mechanical load ¹.

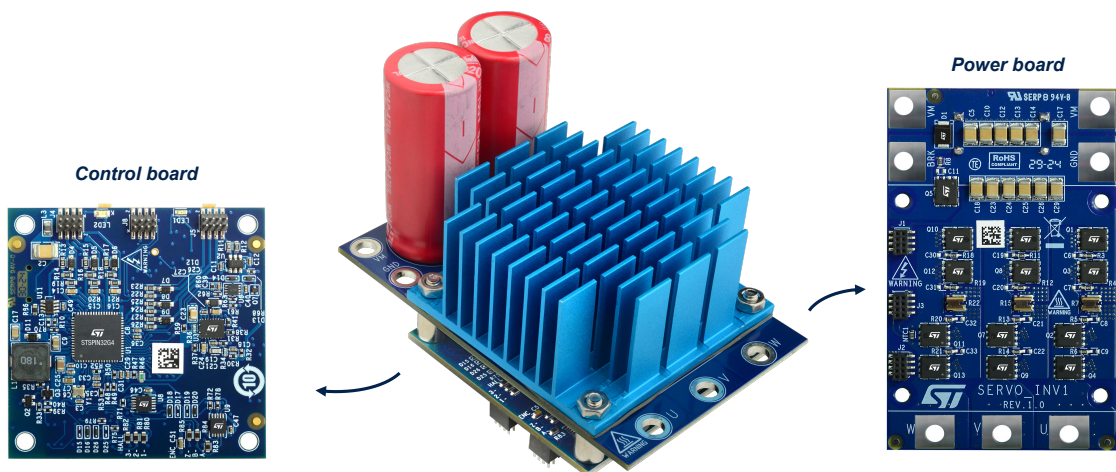
Since these applications commonly use standard industrial voltages such as 24 V and 48 V, their power stages must handle currents of several tens of amperes, leading to critical design challenges from multiple perspectives. Furthermore, this design complexity is exacerbated by recent market trends that favor very compact motor drivers mounted directly on the controlled motor, aiming to reduce cabling, electromagnetic emissions, and cost. In this regard, the sizing of the final transistors composing the power stage and their connection to the servo motor is crucial. Significant current levels may increase power losses and temperatures, as well as overstress board traces, which must be properly addressed ². Additionally, selecting the appropriate control and driver for this power stage plays a key role in ensuring reliable switching behavior and overall robustness of the solution.

To achieve optimal performance from 3-phase brushless motors, advanced control techniques such as Field Oriented Control (FOC) are required, where the magnetic field produced by currents flowing into motor windings is dynamically updated to maximize efficiency. Although these control algorithms have been optimized over the years and are now available for direct implementation on resource-constrained microcontrollers, they still require significant computational power when optimal performance is essential. This can make selecting the best device—balancing performance versus cost—a challenging and time-consuming task.

Considering these factors, the **STSPIN32G4** from STMicroelectronics is well-suited for servo driving solutions, combining in a single, compact, and cost-efficient device: a high-performance STM32 microcontroller, a triple half-bridge gate driver, and flexible power management circuitry. While the microcontroller can manage advanced motor control algorithms and more, the driver fully controls the power stage thanks to its 1-A current capability and integrated protections that detect and mitigate possible fault conditions.

To demonstrate the excellent performance achievable in servo drive applications, STMicroelectronics recently released the **EVLSEURO1** reference design (Figure 1), leveraging the **STSPIN32G4**. Implementation details and performance of the solution are detailed in this document.

Figure 1. EVLSEURO1 reference design

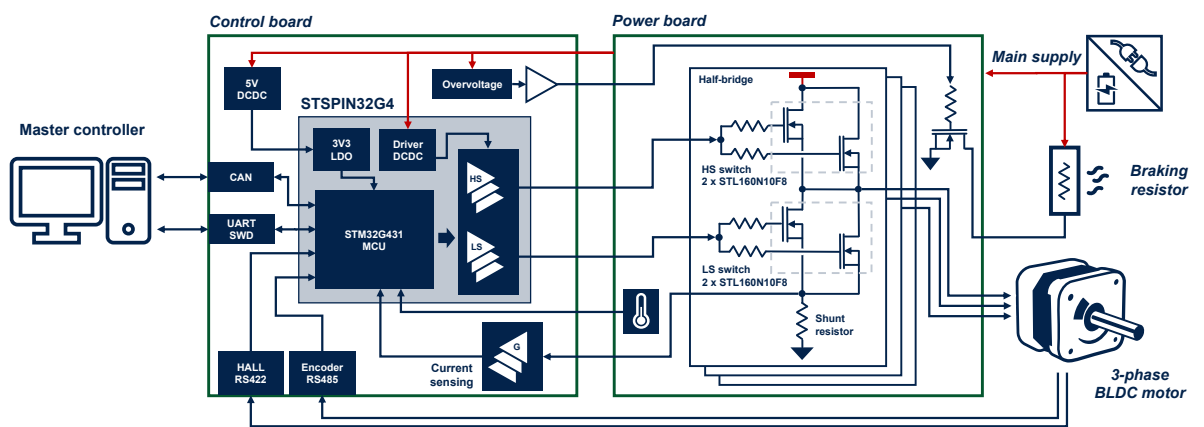


2 Design description

The **EVLSEVVO1** is based on a modular design, as shown in **Figure 1**, consisting of two printed circuit boards (PCBs) stacked together: the control board and the power board. A significant size reduction has been achieved through this partitioning and a smart rationalization of component placement and routing. The result is a board size of only 50 mm (width) × 80 mm (length) × 60 mm (height, including heatsink and bulk capacitors).

The design targets 3-phase brushless DC motors with continuous operating power up to 2 kW with passive cooling or 3 kW using a fan (not included). The system is intended to operate in industrial environments using a nominal bus voltage of up to 48 V; however, it was conceived with a large design margin that extends its operating voltage up to 75 V. The maximum output current to the motor is 63 A_{RMS} or 42 A_{RMS}, respectively, with or without a fan.

Figure 2. EVLSEVVO1 block diagram and connections



3 Power board

With reference to [Figure 2](#), the power board mainly consists of 12 [STL160N10F8](#) MOSFETs arranged in a triple half-bridge configuration. Each switch for the low-side and high-side section is made of two transistors in parallel. Although the selected power MOSFET has a current rating above 100 A, meeting design requirements on its own, this parallel arrangement was adopted to increase efficiency and thermal performance. The overall channel resistance during conduction mode is halved to 1.2 m Ω (typ.), and power losses are split across two separate devices, achieving much better heat distribution on the board surface. Each half-bridge is completed by a 0.5 m Ω shunt resistor, allowing precise measurement of the current flowing through the motor winding via dedicated Kelvin-type connections.

The system provides protection against overvoltage on the bus during regenerative braking. This is a key feature because when the servo driver is requested to reduce operating speed, the control algorithm adjusts the modulation applied to the motor to reverse the power transfer. Normally, when the motor is accelerating or rotating at constant speed, electrical power is supplied to the mechanical load connected to the motor. However, during the deceleration phase, the energy stored in the mechanical system due to its inertia must be removed. During deceleration, the control algorithm drives the motor to behave as a generator so that mechanical power from the load is converted into electrical power and transferred to the servo drive electronics.

When the [EVLSEVO1](#) is part of an environment supporting regenerative braking, this generated power can be transferred through the main bus connection to other appliances, batteries for later reuse, or other servo drivers whose motors require power for their loads during that specific timeframe. Thanks to this power reuse, energy efficiency is improved since the net power requested from the main supply is reduced on average. [EVLSEVO1](#) is fully protected against risks that might arise when the power from regenerative braking is not completely used by other systems. In this case, the main bus voltage increases because the extra energy is temporarily stored in system bulk capacitors, risking an overvoltage condition that could exceed the maximum allowed rating and lead to permanent damage. There is no such risk with [EVLSEVO1](#), as the board allows dissipation of the extra energy in an external power resistor to keep bus voltage within allowed limits and guarantee functionality and precise motor control even in this critical scenario.

Practically, when bus voltage exceeds a selectable threshold, a dedicated MOSFET on the power board is activated on demand by the microcontroller or by a protection circuit and connects the external resistor between the supply bus and ground, completely removing the potential risk.

In designing [EVLSEVO1](#), STMicroelectronics also focused on board layout to achieve high quality. The power board is a 4-layer PCB, where one internal layer is reserved for a solid ground plane to mitigate radiated emissions, while the others are used for signal and power routing ⁴. Regarding manufacturing, an increased copper thickness of 140 μm (4 oz/ft²) was used to guarantee a proper cross-sectional area for power traces and thus reduce parasitic impedance and resistance ². In particular, the output traces connecting to motor windings were replicated on three different layers of the board and interconnected through multiple via holes. All surface-mount components were placed on one side of the board, leaving room on the opposite side for the heatsink and electrolytic bulk capacitors. Dedicated plated holes are available for solid and effective wiring with the motor, the power supply, and the external braking resistor, using cable lugs secured via M4 screws.

4 Control board

The **STSPIN32G4** is the core of the control board, as illustrated in [Figure 2](#). The device executes the control algorithm on the embedded high-performance **STM32G431** microcontroller featuring a Cortex®-M4 core and running at a clock frequency of up to 170 MHz. The microcontroller is programmed through an SWD interface and interacts with the integrated gate driver via dedicated internal connections to generate proper modulation for the motor.

The control board uses 35 µm (1 oz/ft²) copper, allowing for smaller clearance and higher layout density compared to the power board. The control and power boards mate via three dedicated board-to-board connectors for provisioning of supply input, MOSFET gate voltages, power outputs, and shunt resistor signals. These connectors provide an effective method to reduce the solution size thanks to the stacked board design, but they introduce parasitic inductance and resistance along the paths, whose effects must be checked to ensure stability in switching behavior ⁴.

The system provides bidirectional sensing of motor currents as required by FOC control. Sensing is performed via the voltage drop across the three shunt resistors—one for each motor phase—which is amplified by a gain stage based on operational amplifiers. This stage uses a differential configuration, which amplifies the small signals of a few millivolts produced by current flowing through the shunt resistors while rejecting unwanted common-mode noise generated during commutation ³. The amplified signals are then sampled and converted by two 12-bit ADCs within the **STSPIN32G4**.

The gate driver interfaces with the power stage MOSFETs through a biasing network for the gates based on resistors and diodes. This network was tuned to target a slew rate of the output voltage close to 1 V/ns, providing an optimal balance between speed and radiated emissions. Furthermore, the gates of the two MOSFETs in parallel composing each switch were decoupled via two resistors to mitigate and dampen possible instability during commutation ⁵.

The control board leverages the flexible power management circuitry embedded in the **STSPIN32G4**, integrating one buck converter for generating the gate driver supply rail from the main supply voltage and one LDO regulator to supply both the embedded microcontroller and other external circuits in the 3.3 V domain. For efficiency reasons, the LDO regulator is cascaded to an additional 5 V supply generated by an external DC-DC converter, the **L3751**.

The control board allows sensing of motor position via two input sources simultaneously to increase robustness and precision: Hall-effect-based position sensors and an encoder can be connected at the same time. The encoder can be either quadrature type, providing incremental positioning data, or absolute type using SPI or UART interfaces. The board design mitigates potential issues caused by noisy industrial environments, as position inputs are equipped with differential transmitter/receiver circuits compliant with RS422 and RS485 standards, making them extremely rugged.

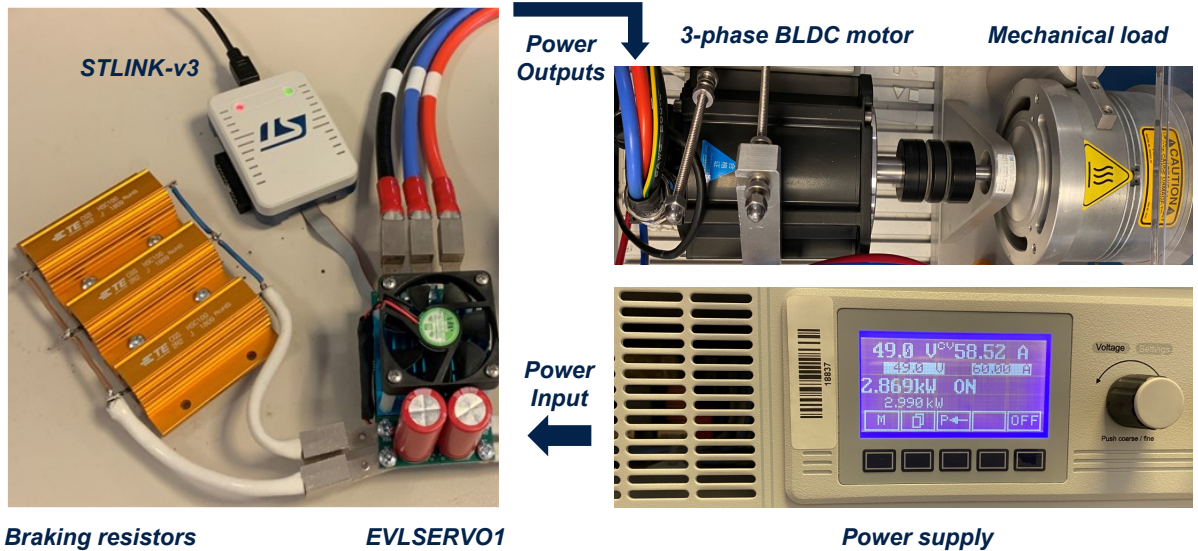
External equipment and controllers can interface with the **EVLSEVO1** through the CAN bus or serial communication.

Finally, the system includes a full set of protections to bring the servo drive and motor to a safe condition in case of overheating (via direct monitoring of power stage temperature), overcurrent, short circuit (via monitoring of the voltage drop across each switch), and overvoltage.

5 Performance

To provide evidence of the robustness and performance of the **EVLSEVO1**, the setup shown in **Figure 3** was used.

Figure 3. EVLSEVO1 driving high power load



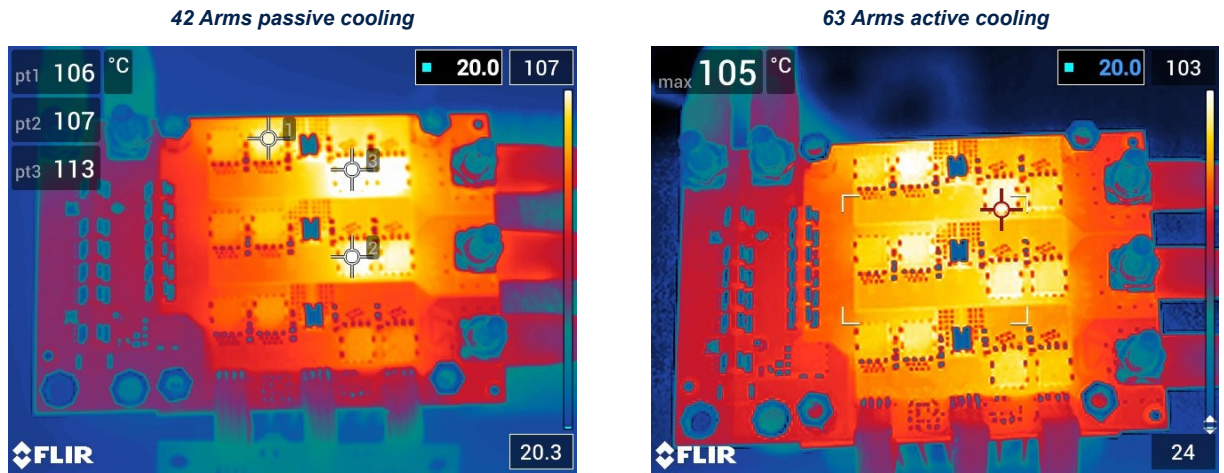
The system's main input was connected to a DC power supply capable of sourcing electric power up to 3.5 kW, while the three outputs were connected to a 3-phase BLDC motor that can deliver a mechanical power of 4.47 kW (6 HP) when rotating at 3000 rpm. The mechanical power from the motor is dissipated via a hysteresis brake. The motor is coupled via a flexible joint. A parallel arrangement of three power resistors was connected as a braking resistor with an overall resistance of roughly 0.9 Ω , considering the wiring to the board. This resistor configuration allows dissipation of a continuous power of 300 W and a peak power up to ten times higher in case of pulsed usage. For example, 3 kW can be dissipated for 3 s, provided pulses are sufficiently delayed to allow resistor cooling.

Leveraging the simplicity of the evaluation ecosystem, the **STSPIN32G4** was configured with firmware implementing the FOC control algorithm, automatically generated through the STMicroelectronics **MCSDK** tool suite based on motor parameters and board configuration (16 kHz switching frequency, 48 V nominal bus voltage, 12 V gate driver voltage). The servo drive was programmed and controlled directly by computer via an **STLINK-V3** debugger featuring SWD and Virtual COM port to the microcontroller. This setup enabled real-time changes to motor speed and torque and monitoring of drive status (temperature, voltage, protections, and faults) through the Motor Pilot GUI included in the **MCSDK**.

The **EVLSEVO1** was pushed to its maximum operating limits, managing an average power close to 3 kW, as shown on the power supply display in **Figure 3**. To dissipate heat generated by the power stage under these conditions, a fan was mounted on top of the **EVLSEVO1** heatsink, producing an airflow of 12 m³/h.

With normal assembly, the MOSFETs are hidden from view due to control board mating. For deep analysis of their actual temperature evolution, the power board and control board were rearranged side by side in a coplanar configuration using custom wiring. This allowed thermal camera imaging of the power board, as shown in **Figure 4**. Initially, the fan was turned off, and the motor was running with sinusoidal currents of 42 A_{rms}. The system reached steady state after approximately 15 minutes in an environment at about 25°C. The hottest point on the board was a low-side MOSFET that reached 113°C, as visible on the left side of **Figure 4**. After this test, the fan was turned on, and the output current was increased to 63 A_{rms}. In this condition, the maximum temperature of the same MOSFET decreased to 105°C, as shown on the right side of **Figure 4**. This temperature decrease was due to the significant reduction in board-to-ambient thermal resistance provided by forced airflow.

The selected BOM can easily accommodate the expected temperature increase when the two boards are stacked together, which reduces the air gap and affects convective heat exchange. In fact, **STL160N10F8** MOSFETs allow for a junction temperature up to 175°C, ensuring a significant design margin and safe operation of the drive at full power.

Figure 4. Thermal imaging of EVLSERVO1 power board


The switching performance of the inverter was also evaluated while operating from zero to the maximum current, as reported in Figure 5. Each of the six graphs in Figure 5 shows the most significant signals associated with the commutation of one of the three half-bridges, with the other two half-bridges exhibiting comparable behavior. Reported signals are:

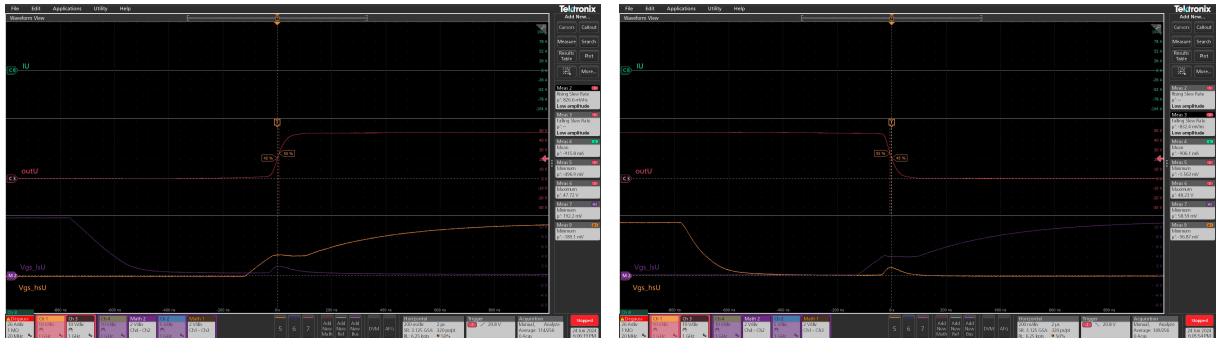
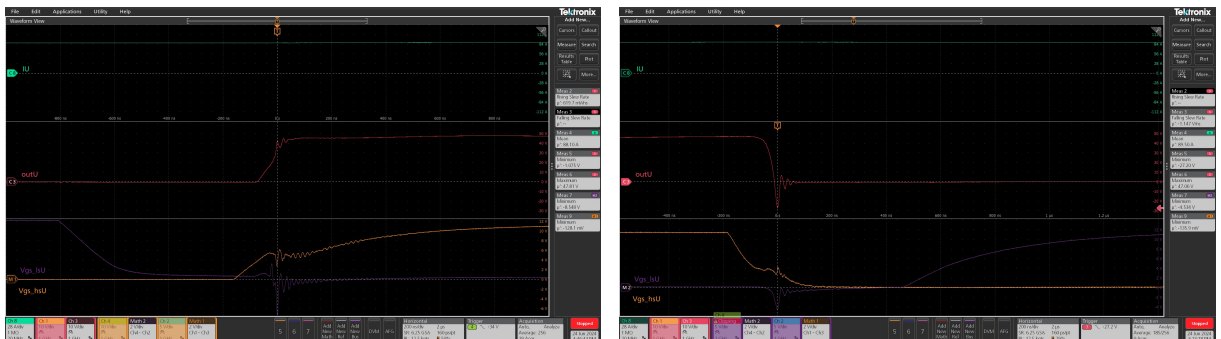
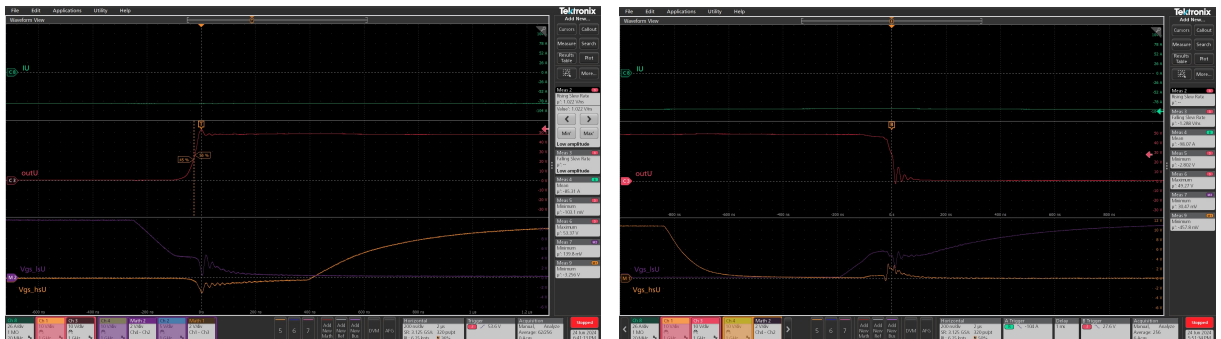
1. I_U — the current flowing out of the U half-bridge
2. out_U — the voltage of the output node for the U half-bridge
3. V_{gs_lsU} — the gate-to-source voltage for one of the two paralleled low-side MOSFETs in the U half-bridge
4. V_{gs_hsU} — the gate-to-source voltage for one of the two paralleled high-side MOSFETs in the U half-bridge

All voltage signals were measured using short ground springs for oscilloscope probes to minimize both noise injection from parasitic field coupling via the ground loop antenna and parasitic lead inductance ⁶.

As evident from the first row in Figure 5, the commutation at zero load current was very clean in terms of MOSFET voltages and output voltage, with the latter exhibiting a rising and falling slew rate of roughly 0.83 V/ns. Sometimes, even with the most careful layout process, parasitic inductance inside power stage paths can produce oscillations due to large and sudden current variations that this solution must manage. This might explain the perturbations observed on the measured voltages when the output current reached its maximum peak value of around 90 A (second and third rows in Figure 5). Nevertheless, thanks to the robustness of the STSPIN32G4 and the selected power MOSFETs, these values are not of concern.

In particular, the maximum overshoot of the output voltage was around 5.3 V, observed at the rising edge of the low-side hard-switching case where commutation is controlled by the low-side switch turning off. Regarding the maximum below-ground voltage, it was measured at roughly -27 V during the falling edge of the high-side hard-switching case where commutation is controlled by the high-side switch turning off. This effect was mitigated by the board-to-board connectors between the power and control boards, which filtered the below-ground voltage to roughly -10 V when reaching the STSPIN32G4. In all other cases, the signals between the control and power boards did not show significant misalignment.

Finally, the maximum positive and negative slew rates for the output node were measured during low-side hard switching at about 1 V/ns and -1.3 V/ns, respectively, closely matching the desired target values.

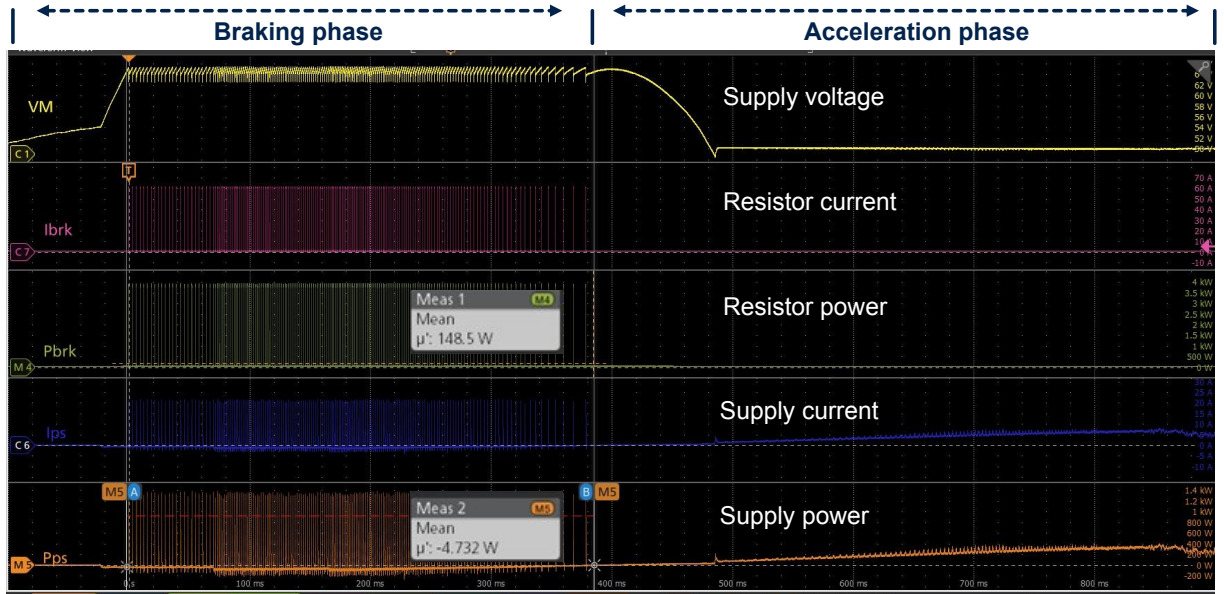
Figure 5. EVLSERVO1 commutations of power MOSFETs
Zero current switching

High Side hard switching

Low Side hard switching


An example of intervention for the braking resistor is shown in [Figure 5](#). In this case, the mechanical brake was disabled so that no significant power was dissipated, except for friction losses, while the mechanical inertia of the setup was exploited to store energy during rotation. The motor was running in the clockwise direction, then the drive was commanded to suddenly reverse the shaft rotation to counterclockwise to stimulate regenerative braking.

As seen in [Figure 5](#), there is an initial phase where the bus voltage increases because the motor behaves as a generator and injects current into the bulk capacitors of the system. Since a single-quadrant power supply was used during the test and no other appliance was connected to sink and use this extra power from regenerative braking, the bus voltage exceeded the programmed intervention threshold, and the protection circuitry engaged to dissipate this power through the braking resistors. During the entire braking phase, the resistors were activated multiple times in pulsed mode so that the bus voltage was clamped in a safe range between 62 V and 65 V.

In this braking test, the pulsed current reached 60 A, leading to a peak power of roughly 3.4 kW and an average power of 148 W. During the braking phase, the **EVLSERVO1** supplied an average power of around 4.7 W to the power supply, just to charge bulk capacitors inside the equipment. Then, the motor reversed its direction and started accelerating counterclockwise with power from the supply progressively increasing up to 400 W to reach the target speed.

Figure 6. Intervention of braking resistor



6 Conclusion

In this paper we examined the [EVLSEVO1](#) reference design that was recently released by STMicroelectronics. The design addresses the servo drive segment and is based on the [STSPIN32G4](#), advanced motor control device. Notably the [EVLSEVO1](#) can drive 3-phase BLDC motors with a power up to 3 kW, with very good switching and thermal performances of the power stage. Its reduced form factor obtained thanks to the modular board approach, enables for relocation of the electronics close to the motor as desirable in servo drive applications. Several protections are available, among which a dedicated circuitry to manage possible bus overvoltage due to regenerative braking, for a robust design under fault conditions. All this definitely makes [EVLSEVO1](#) a perfect suit for reliable and effective motor control in high-power and low-voltage solutions.

7 References

1. Servo motor driver design for high performance applications, IEEE paper
2. TA0361 - Thermally aware high-power inverter board for battery-powered applications, Technical article
3. AN5397 - Current Sensing in motion control applications, Application note
4. AN4694 - EMC design guides for motor control applications, Application note
5. Design rules for paralleling of Silicon Carbide Power MOSFETs, Conference paper
6. Why Do Passive Oscilloscope Probes Have So Many Ground Connection Options?

Revision history

Table 1. Document revision history

Date	Version	Changes
13-Jan-2026	1	Initial release.

Contents

1	Introduction	2
2	Design description	3
3	Power board	4
4	Control board	5
5	Performance	6
6	Conclusion	10
7	References	11
	Revision history	12

List of figures

Figure 1.	EVLSERVO1 reference design	2
Figure 2.	EVLSERVO1 block diagram and connections	3
Figure 3.	EVLSERVO1 driving high power load	6
Figure 4.	Thermal imaging of EVLSERVO1 power board	7
Figure 5.	EVLSERVO1 commutations of power MOSFETs	8
Figure 6.	Intervention of braking resistor	9

List of tables

Table 1. Document revision history 12

IMPORTANT NOTICE – READ CAREFULLY

STMicroelectronics NV and its subsidiaries (“ST”) reserve the right to make changes, corrections, enhancements, modifications, and improvements to ST products and/or to this document at any time without notice.

In the event of any conflict between the provisions of this document and the provisions of any contractual arrangement in force between the purchasers and ST, the provisions of such contractual arrangement shall prevail.

The purchasers should obtain the latest relevant information on ST products before placing orders. ST products are sold pursuant to ST’s terms and conditions of sale in place at the time of order acknowledgment.

The purchasers are solely responsible for the choice, selection, and use of ST products and ST assumes no liability for application assistance or the design of the purchasers’ products.

No license, express or implied, to any intellectual property right is granted by ST herein.

Resale of ST products with provisions different from the information set forth herein shall void any warranty granted by ST for such product.

If the purchasers identify an ST product that meets their functional and performance requirements but that is not designated for the purchasers’ market segment, the purchasers shall contact ST for more information.

ST and the ST logo are trademarks of ST. For additional information about ST trademarks, refer to www.st.com/trademarks. All other product or service names are the property of their respective owners.

Information in this document supersedes and replaces information previously supplied in any prior versions of this document.

© 2026 STMicroelectronics – All rights reserved